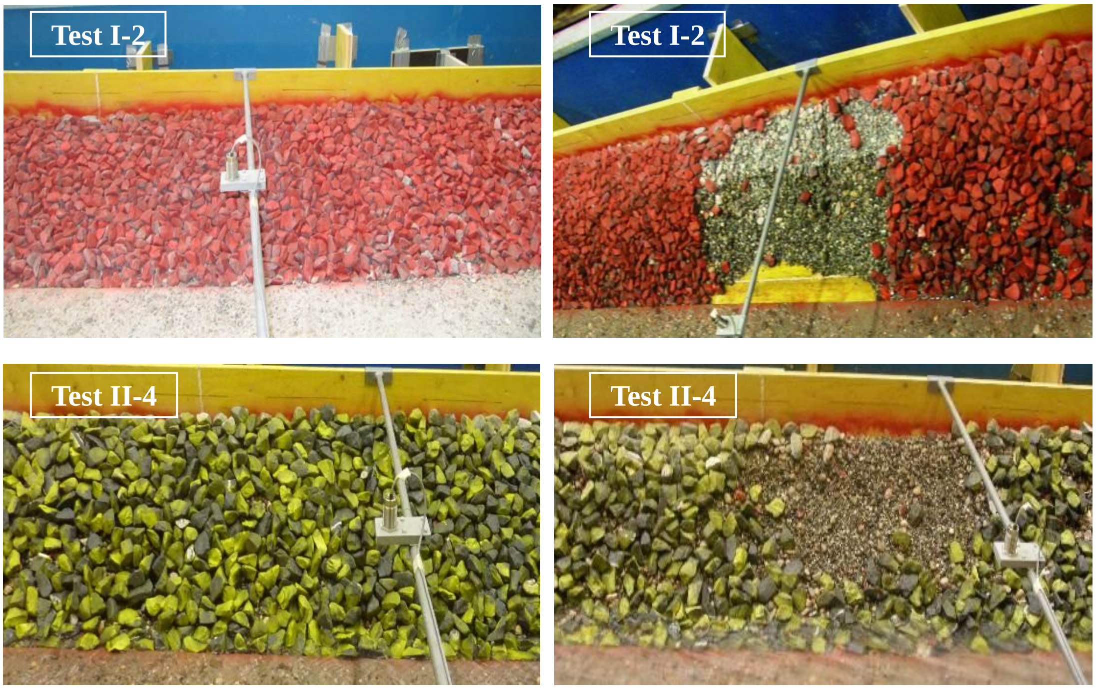

(a) **(b)**

Figure 3 Riprap before (a) and after (b) failure for tests I-2 and II-4 (see table 2).

Figure 4 shows the time evolution of the cumulated number of eroded blocks. Time of failure (t_f) is normalized by the duration of the tests $T_{\max}$=180:

$$t^* = \frac{t_f}{T_{\max}} \tag{2}$$

Failure corresponding to the abrupt change of the slope of the graphic in Figure 4 is related to the transport of the material causing in the total failure of a bank protection.

Figure 4-(a) shows the series of tests in group I which included six different discharges. It can be observed that gradually increasing the constant discharge of the test I-1 to I-6 has an impact on the time of failure. Two of the tests in this group reached total failure and the critical unit discharge for this specific size compared to a value between q=0.249 m^2/s and q=0.262 m^2/s and with a failure time of roughly 1 hour and 30 minutes after beginning of the test. An increase of 14.9% of the unit discharge (to q=0.301 m^2/s), resulted in an earlier failure (-17%).

In Figure 4-(b) shows the data of of 7 different tests for medium size blocks. The significant impact of increasing discharge on the time of total failure and amount of eroded blocks can be clearly seen. Herein, the first total failure occurs for q=0.407 m^2/s at 90% of maximum time of the experiments (1hour and 42 minutes). Thus by increasing the unit discharge of 3.3%, 5.6%, 8.6%, and 16.2% the time of failure was reduced, 23%, 57%, 82%, and 87% respectively.

For largest blocks (d_B=0.047 m), failure condition was reached only for the test III-1 (q=0.480 m^2/s). Figure 4-(c) indicates that the largest size of blocks (0.047 m) delayed the failure for a higher discharge by 15.2% as compared to the medium size and by 45.4% compared to the small sized blocks. For similar unit discharge the rate of block erosion is decreased by increasing the size of the riprap. Figure 4-(d) gives the comparison between one layer and two layers erosion rate for the same unit discharge. The second layer (lower layer) postponed the failure of the section significantly, namely around 50% of the total experiment duration. However the rate of erosion of upper layer is higher.

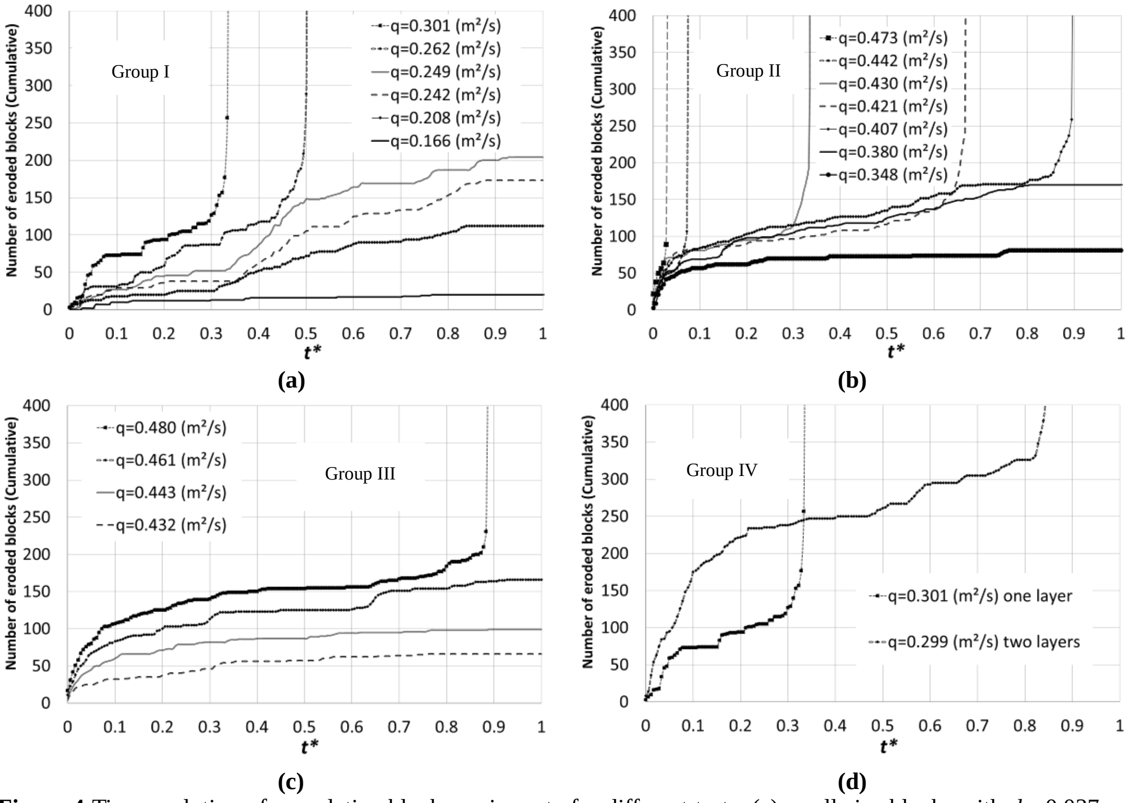

Figure 4 Time evolution of cumulative block erosion rate for different tests: (a) small size blocks with d_B=0.037 m; (b) medium size blocks with d_B=0.042 m; and large size blocks with d_B=0.047 m; (d) comparison of block erosion between one layer and two layers of riprap in size of d_B=0.037m

In Figure 5 the relationship between dimensionless failure time t^* and (a)velocity, (b)Froude number, (c)bed shear stress and (d) dimensionless bed shear stress or Shields factor of one layer tests (group tests of I to III) is presented.

Figures 5-(a) to 5-(c) show the similarity and the results for the different block diameters apparently are in a same pattern. A plateau at t^*=1, corresponding to tests with no failure, is interpreted by a sudden decrease in the t^* values, corresponding to tests with failure. Results are grouped by block size. Nevertheless, for each block size, clear limit values above which failure of the riprap protection is expected exist for mean velocity, Froude number and bed shear stress,.

In terms of velocity, failure of the riprap is expected for small, medium and large sizes blocks for values above roughly 2.0, 2.4 and 2.6 m/s, respectively. For Froude number and bed shear stress, threshold limit limits are roughly lower than 1.68 and 43 Pa for small d_B, around 1.81 and 53 Pa for medium d_B and more than 1.88 and 58 Pa for large one. Curves corresponded to t^* should converge asymptotically to t^*=0. When any of these parameters increases, the fact can be inferred from the shape on the lower part of the curves for medium size block results.

In Figure 5-(a) to 5-(c) the failure time and consequently the occurrence of failure as a function of inertial flow resistance forces and block diameter is shown. Normalization of bed shear stress shows the similarity of the results in terms of failure time as seen in Figure 5-(d). This dimensionless bed shear stress also represents the balance of hydrodynamic forces acting on the riprap and the submerged weight of the blocks. Dimensionless shear stress is calculated as follows:

$$\tau^* = \frac{\tau}{(S_B - 1) g \rho d_B} \qquad (3)$$

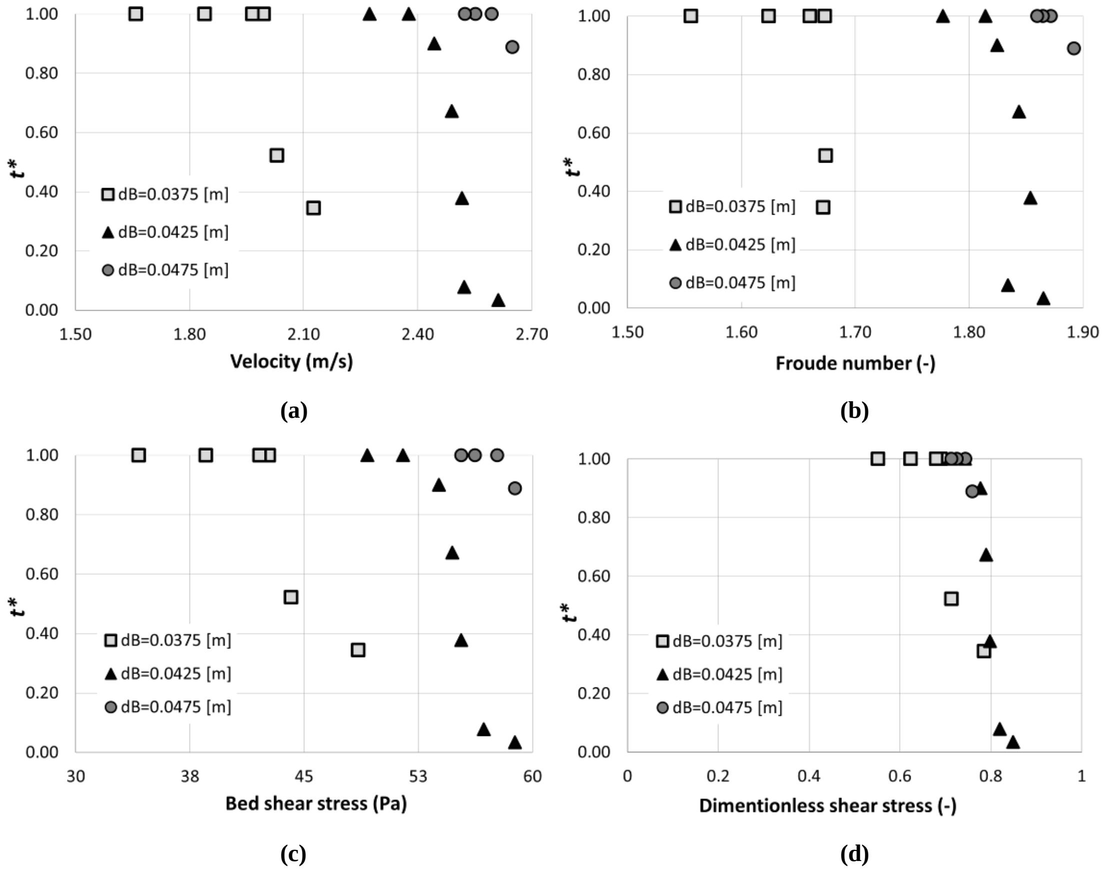

Figure 5 Normalized failure time versus mean velocity (a), Froude number (b), bed shear stress (c), and dimensionless shear stress (d)

where τ is the shear stress, S_B is the specific gravity of rocks, g is the gravitational acceleration, ρ is water density and d_B is the size of blocks. Figure 5 represents that the results of all groups of one layer tests that have the same trend regardless the size of rock blocks.

It can be also witnessed that the normalized time as t*=1 characterizes the equilibrium which means that the riprap can stay stable regardless the time changes (considering the scaled model).

4 CONCLUSIONS

The behaviour of compressed, well positioned riverbank protection riprap was analysed in this research, considering the influence of size of blocks and thickness of riprap layer. Time dependent analysis of failure was performed. The maximum three hours duration of the flume tests can cover roughly 15 hours of an extreme event by taking into account a typical geometry scale factor between the experiments and actual Swiss mountain rivers.

A remarkable relationship between the size of riprap and the time of failure was observed. Furthermore, not only the larger block sizes postponed the time of failure but also reduced the block erosion rate significantly. By considering the two layer test, first results revealed that under the same conditions, the second layer stabilizes the protection system significantly and delays the time of total failure. Nevertheless, the erosion rate of the upper layer of rock blocks increased.

ACKNOWLEDGEMENT

The research project is supported by Swiss Federal Office for the Environment (FOEN) under contract no. A2111.0239/10-0019.PJ/J372-1192.

References

Abt, S.R., Thornton, C.I., Gallegos H.A., and Ullmann C.M. 2008. Round-shaped riprap stabilization in overtopping flow. Journal of Hydraulic Engineering 134(8): 1035.

Brown, S.A. and Clyde, E.S. 1989. Design of riprap revetment. Hydraulic Engineering Circular No. 11, Federal Highway Administration, McLean, VA.

California Division of Highways (CDH). 1970. Bank and shore protection in California highway practice. Sacramento, CA: California Department of Public Works.

Center for Civil Engineering Research and Codes (CUR). 1995. Manual on the use of rock in hydraulic engineering. Rotterdam, Netherlands: Balkema.

De Almeiada, G. A. M., and Martin-Vide, J. P. 2009. Riprap stability: Transverse and longitudinal versus continues protections, J. Hydraul Eng. 135:447-456.

Escarameia, M. and May, R.W.P. 1992. Channel protection downstream of structures. Rep. SR 313. London: HR Wallingford.

Froehlich, D.C. and Benson C.A. 1996. Sizing dumped rock riprap. Journal of Hydraulic Engineering, ASCE 122(7): 389–396.

Froehlich, D.C. 2011. Sizing loose rock riprap to protect stream bank. River Research and Application. Published online in Wiley Online Library, (wileyonlineliberary.com).

García H.M. (ed.) 2007. Sedimentation Engineering: Processes, Measurements, Modeling, and Practice. Reston, VA: American Society of Civil Engineering.

Grace, J.L. Jr., Calhoun C.C. Jr., and Brown D.N. 1973. Drainage and erosion control facilities: Field performance investigation. Miscellaneous paper H-73-6, US Army Engineer Waterways Experiment Station, Vicksburg, MS.

Jafarnejad, M., Pfister, M, Schleiss, A. J., 2012. Failure risk analysis of riverbank ripraps with Monte Carlo simulation. River Flow 2012, Taylor and Francis Group, 1325-1330.

Julien, P.Y. 2002. River mechanics. London: Cambridge University Press.

Lagasse, P.F., Clopper, P.E., Zevenbergen, L.W., Ruff, J.F. 2006. Riprap design criteria, recommended specifications, and quality control. Washington, DC: National Cooperative Highway Research Program.

Li, R.M., Simons, D.B., Blinco, P.H., Samad, M.A. 1976. Probabilistic approach to design of riprap riverbank protection. Rivers 76 Symposium on Inland Waterways for Navigation, Flood Control, and Water Diversions, Vol. I: 1572–1591. Fort Collins, CO: American Society of Civil Engineering.

Maynord, S. T.,Ruff, J. F., and Abt, S. R., 1987. Riprap design. J. Hydraul. Eng., 115, 937-949.

Permanent International Association of Navigation Congress (PIANC). 1987. Risk consideration when determining bank protection requirements. Report of Permanent Technical Committee 1, Supplement to Bulletin 58. Brussels, Belgium: PIANC.

Racin, J.A. 1996. California bank and shore rock slope protection design: Practitioner's guide and field evaluation of riprap methods. Final Rep. FHWA-CA-TL-95-10, Caltrons Study F90TL03, Sacramento, Calif.

Reese, A. 1984. Riprap sizing four methods. Proceedings of the ASCE Hydraulics Division Specialty Conference. New York: ASCE.

Schleiss, A.J. 2000. Bemessung und Gestaltung von Blockwürfen an Gebirgsflüssen. Interpraevent. Villach. Tagungspublikation, Band 2, S. 351-360.

Stevens, M.A., Simons D.B., and Lewis G.L. 1976. Safety Factors for Riprap Protection. ASCE Journal of the Hydraulics Division 102(HY5): 637–655.

Stevens, M.A., Simons D.B., and Richardson E.V. 1984. Riprap Stability Analysis. Transportation Research Board, Transportation Research Record 2: 209–216.

Straub, L.G. 1953. Dredge fills closure of Missouri River at Fort Randall. In Proceedings: Minnesota International Hydraulics Convention, September 1-4, 1953, Minneapolis, Minnesota: 61–75. Minneapolis, MN: WM.C. Brown Co.

Ulrich, T. 1987. Stability of rock protection on slopes. ASCE Journal of Hydraulic Engineering 113(7): 879–891.

U.S. Army Corps of Engineering (USACE). 1994. Hydraulic design of flood control channels. EM 1110-2-1601. Washington, DC: US Government Printing Office.

Wittler, R.J., and Abt, S. R. 1988. Riprap design by modified Safety factor method. Proceeding of National Conference on Hydraulic Engineering: 143–148. Colorado Springs, CO: American Society of Civil Engineering